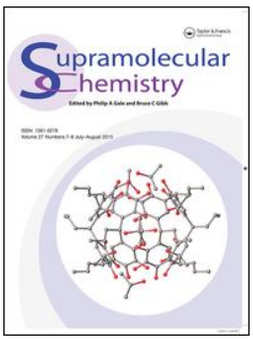

Supramolecular Chemistry

ISSN: 1061-0278 (Print) 1029-0478 (Online) Journal homepage: https://www.tandfonline.com/loi/gsch20

Single-component, low molecular weight organic supergelators based on chiral barbiturate scaffolds

Daniel T. Seidenkranz, Kurt A. Langworthy, Lev N. Zakharov & Michael D. Pluth

To cite this article: Daniel T. Seidenkranz, Kurt A. Langworthy, Lev N. Zakharov & Michael D. Pluth (2019): Single-component, low molecular weight organic supergelators based on chiral barbiturate scaffolds, Supramolecular Chemistry, DOI: 10.1080/10610278.2019.1629437

To link to this article: https://doi.org/10.1080/10610278.2019.1629437

SUPRAMOLECULAR CHEMISTRY
https://doi.org/10.1080/10610278.2019.1629437

Taylor & Francis
Taylor & Francis Group

ARTICLE

OPEN ACCESS Check for updates

Single-component, low molecular weight organic supergelators based on chiral barbiturate scaffolds

Daniel T. Seidenkranz[a], Kurt A. Langworthy[b], Lev N. Zakharov[b] and Michael D. Pluth[a]

[a]Department of Chemistry and Biochemistry, Materials Science Institute, University of Oregon, Eugene, OR, USA; [b]CAMCOR–Center for Advanced Materials Characterization in Oregon, University of Oregon, Eugene, OR, USA

ABSTRACT

We report here the first chiral barbiturate to act as a single-component LMOG capable of gelating a variety of chlorinated and aromatic solvents. Solution-based DOSY NMR experiments, solid-state VP-SEM, and X-ray crystallography techniques were used to characterize chloroform-based gels at a variety of size domains. This scaffold provides a simple system to study the dynamics of gelation and self-assembly.

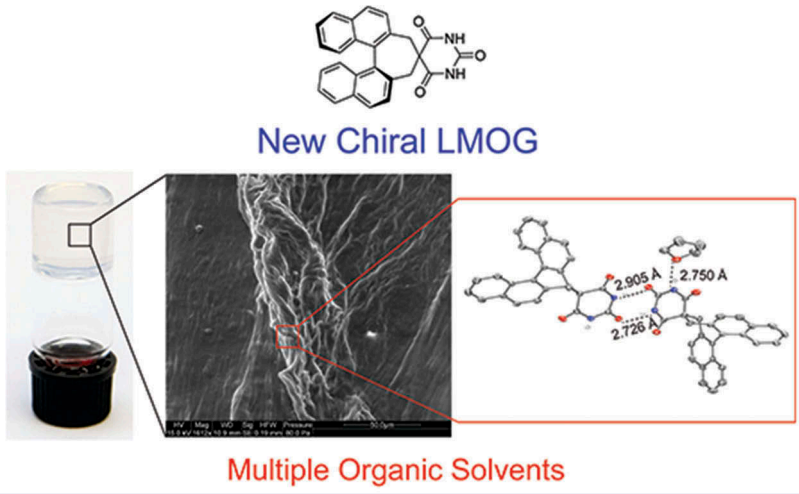

ARTICLE HISTORY
Received 3 March 2019
Accepted 3 June 2019

KEYWORDS
Barbiturates; gelation; self-assembly

Introduction

Supramolecular gels are an emerging class of soft materials with unique and tunable rheological and thermal properties (1). Due to their viscoelastic properties, supramolecular gels capable of gelating organic solvents (organogels) have found widespread application in sensing and stimuli responsive materials (2–13), optoelectronics (14–23), drug delivery/regenerative medicine (24, 25), and as templates for nanoparticles and other inorganic structures (26–28). Structurally, organogelators often range from macromolecular polymeric gelators to single small molecules constituting low molecular-weight organic gelators (LMOGs). In addition, multicomponent gel systems have also been reported (29–32). In LMOGs and multicomponent systems, gel formation typically occurs through the self-assembly of individual units to produce one-dimensional fibers that become three-dimensionally entangled or crosslinked. The delicate balance required to favor gelation over crystallization or dissolution is typically achieved through careful tailoring of the non-covalent interactions to guide self-assembly. These interactions often include H-bonding, π-π stacking, metal-coordination, and/or van der Waals interactions. Here, we report a simple approach to accessing chiral, single-component, supergelators using simple and readily-accessible starting materials.

Among the most popular strategies for creating new organogelators is incorporation of long, single chain alkyl groups or cholesteryl moieties to a specific scaffold of interest (29, 33). Another popular motif for the construction

CONTACT Michael D. Pluth pluth@uoregon.edu Department of Chemistry and Biochemistry, Materials Science Institute, University of Oregon, Eugene, OR 97403, USA

Supplemental data for this article can be accessed here.

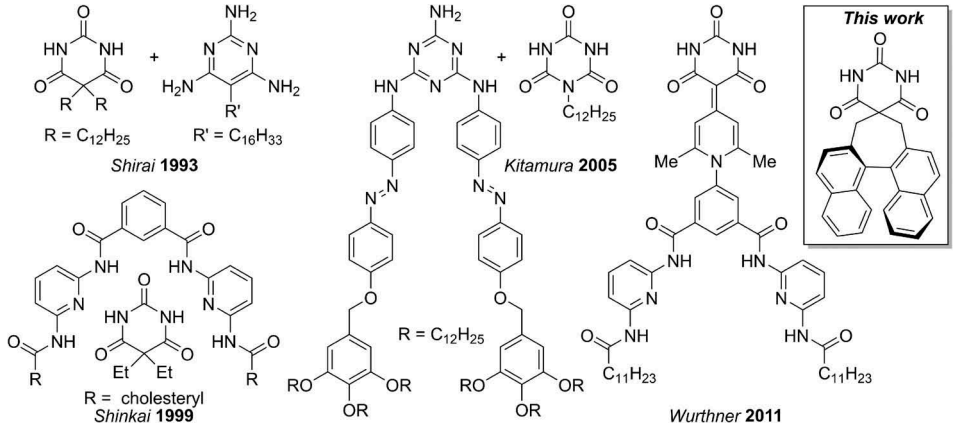

Figure 1. Previously reported organogelators based on the melamine·barbiturate/cyanurate motifs (left) and a new chiral, single-component LMOG based on a barbiturate scaffold (right).

of supramolecular gels is the melamine·barbiturate/cyanurate binary system (Figure 1) (34–38). Such systems are characterized by the complementary donor-acceptor-donor hydrogen bonding motif of the melamine unit, and the acceptor-donor-acceptor motif of the barbiturate/cyanurate. Although these systems show promising gelation behavior, functionalization with long alkyl chains or large cholesteryl groups is required for efficient gelation (37). A rare example of a strategically modified, self-complementary barbiturate/receptor has been reported, but the gelation ability of this system was poor and limited to specific solvent conditions and required a high weight percent (8 wt %) of gelator (39).

Adding to the inherent gelation properties, the inclusion of chirality is also a common feature of organogelators (40, 41). Unfortunately, the useful properties of enantiopure chiral gelators are often eroded when used as racemic mixtures with most racemates showing no gelation behavior. Additionally, by studying the self-assembly of these chiral building blocks, researchers can begin to understand the mechanisms of chirality transfer from single molecules to self-assembled, chiral nanostructures (42–46). Therefore, there is significant interest in developing new chiral organogelators that do not require large alkyl and steroidal groups to induce gelation behavior. Aligned with this need, we report a chiral barbiturate that functions as a single component LMOG in various organic solvents with low loading requirements for gelation (0.3 wt%), which classify it as a supergelator. Notably, this construct lacks the large alkyl chains or cholesteryl groups commonly employed to induce gelation, and instead utilizes a simple, planar chiral, aromatic backbone with a polar H-bonding head group to induce gelation thus providing a versatile platform for future expansion and application.

Results and discussion

Because barbiturates are capable of forming large hydrogen bonding networks, we reasoned that incorporation of chiral groups could provide access to homochiral self-assembled networks. To provide additional and complementary molecular interactions to the hydrogen bonding barbiturate core, we chose to incorporate aromatic subunits to provide the potential for additional long-range order through π-stacking interactions. Combining these design principles, we reasoned that use of axially-chiral binaphthyl (BINAP) groups could be used to increase molecular complexity. To prepare the target barbiturate, we treated barbituric acid with the *bis*(methylbromide) of BINAP to prepare enantiopure BINABarb (Figure 2(a)).

Upon preparation of **1**, we observed that dilute CH_2Cl_2 solutions formed gels, whereas similar solutions of benzyl barbiturate (**3**) failed to gelate. Building from these initial observations, we sought to determine the gelation ability of **1** towards other organic solvents and compare this to structural analogues of **1** (Figure 2(b)). The results from the screening show that **1** forms organogels in different chlorinated solvents (Table 1, Entries 1–4) and substituted aromatic solvents (Table 1, entries 8–11). Solvents such as tetrachloroethane, CCl_4, and benzene showed no gelation behavior suggesting a fine balance between solubility, crystallization, and gelation. The apparent trend that requires at least one substituent on the aromatic ring for gelation is unusual and is currently under further investigation in our laboratory. Solvents containing either hydrogen bond accepting or donating groups eroded the gelation behavior, which is consistent with the requirement of a barbiturate hydrogen bonding network for successful gelation. In addition, we probed the potential gelation

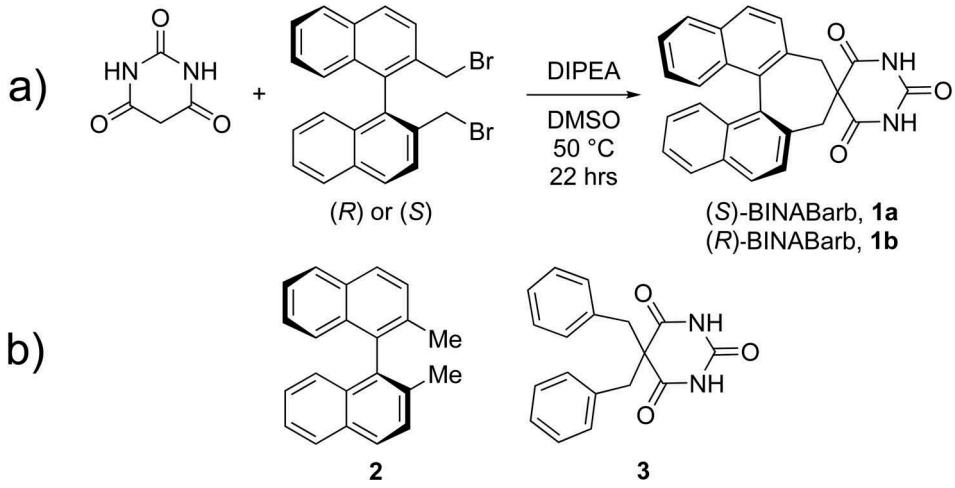

Figure 2. a) Synthesis of (S)/(R)-BINABarb from barbituric acid with (S)-stereochemistry shown. b) Structures of control compounds that are not organogelators.

Table 1. Gelation properties of compounds 1–3 at r.t. G = gel, S = soluble, ppt = precipitate formed, SS = slightly soluble, I = insoluble.

entry	solvent	1a	2	3
1	chloroform	G	S	S
2	chlorobenzene	G	S	ppt
3	dichloromethane	G	S	SS
4	dichloroethane	G	S	S
5	tetrachloromethane	I	S	ppt
6	tetrachloroethane	S	S	S
7	benzene	I	S	ppt
8	toluene	G	S	ppt
9	o-xylene	G	S	ppt
10	m-xylene	G	S	ppt
11	p-xylene	G	S	ppt
12	nitrobenzene	S	S	S
13	pyridine	S	S	S
14	tetrahydrofuran	S	S	S
15	ethyl acetate	S	S	S
16	acetone	S	S	S
17	acetonitrile	S	S	S
18	ethanol	ppt	S	S
19	methanol	ppt	S	S
20	water	I	I	ppt

behavior of structurally-similar compounds **2**, which contains the BINAP moiety but lacks the barbiturate, and in **3**, which contains the barbiturate but lacks the BINAP moiety, and failed to observe gelation behavior of either of these compounds in any of the solvents investigated.

To investigate the self-assembly of BINABarb on the molecular level we performed diffusion-ordered NMR spectroscopy (DOSY) on compounds **1–3** in $CDCl_3$. We hypothesized that if significant self-assembly was occurring, then a significant change in the diffusion coefficient could be measured. Using this technique also provided another opportunity to elucidate some of the structural requirements for gelation by comparing the diffusion coefficients of **1** to structural analogues **2** and **3**. The effects of gelator concentration on diffusion coefficient for **1a** and control compounds **2** and **3** are shown in Figure 3. The sharp break in the measured diffusion coefficient of **1a** is indicative of significant self-assembly and the formation of higher order nanostructures (47, 48). The minimum gelation concentration was observed to be 10 mM or 0.3 wt%, which classifies **1a** as a supergelator (49). Increasing the concentration beyond the minimum gelation concentration (15–25 mM) showed no significant change in diffusion coefficient. Gelation was also confirmed for all samples > 10 mM by a simple inversion test. The critical gelation temperature (T_{gel}) for **1a** was also measured using VT-DOSY and found to be ~50°C. In addition, VT-DOSY confirmed the thermal reversibility of the self-assembly (Figure S6). In contrast, neither **2** nor **3** show any significant change in diffusion coefficient within a similar concentration regime. These results support the necessity of both a polar head and an aromatic tail for self-assembly to occur. Additionally, the biphenyl derivative of BINABarb shows no gelation properties and could not be further studied due to poor solubility in the required concentration regime. Therefore, we attribute the unique gelation behavior observed by **1a** and **1b** over other barbiturates to the inherent chirality of the binaphthyl backbone, which allows for extension of the individual molecular units into an extended nanostructure. Attempts to measure racemic mixtures of the barbiturate at concentrations above 10 mM resulted in precipitation rather than gel formation, further suggesting that the chiral backbone is critical to gelation.

In an effort to understand key interactions at the molecular level that could be responsible for the gel formation of **1**, we turned to x-ray crystallography. Attempts to grow single crystals from dilute solutions of chloroform or other solvents that induced gelation were unsuccessful, highlighting the propensity of these systems to gelate rather

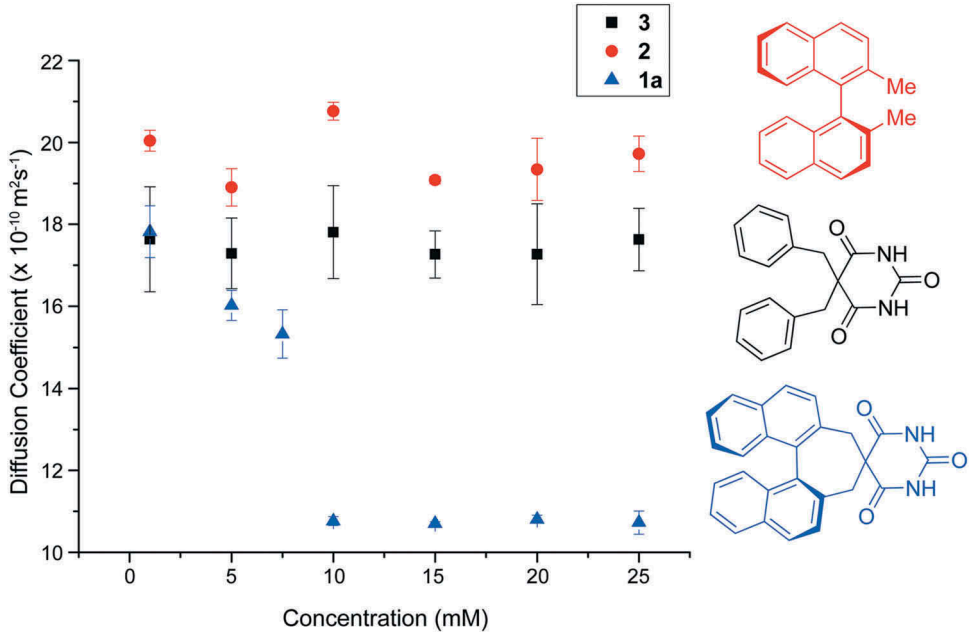

Figure 3. Plot of diffusion coefficient vs barbiturate concentration in $CDCl_3$ at 25°C. Values reported are an average of at least 3 independent trials (± σ).

than crystallize. We were, however, able to grow crystals of **1b** from THF/pentane vapor diffusion. Although these were not the gelation conditions and may not reflect the exact interactions present in the gels, we surmised that analysis of the crystallographic details could provide additional information on the types of intramolecular interactions present in these systems. Analysis of the crystal structure shows clear dimerization between the two pyrimidine heads with the other hydrogen bonds satisfied by a THF co-solvent (Figure S7). Expansion of the asymmetric unit shows long range order, driven by hydrogen bonding and π-stacking, that could result in helical fiber formation upon gelation as observed in the VP-SEM experiments (Figure 4). The barbiturate polar head groups are held together by H-bonding interactions between a neighboring barbiturate and the THF co-solvent, while there is a short, T-shaped contact (3.451 Å) between the aromatic π-faces of the binaphthyl backbone in neighboring columns. This arrangement leads to the formation of two intertwining chains that could explain the helicity of the fibers formed in solution. It can also then be rationalized why polar solvents inhibit gel formation. Erosion of the hydrogen

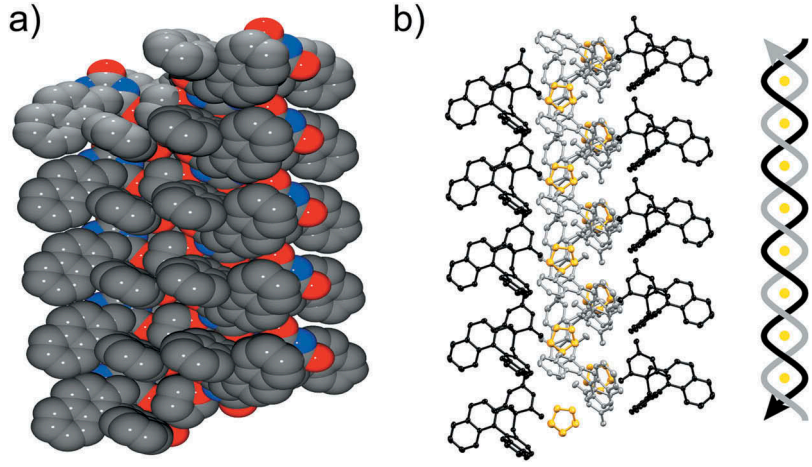

Figure 4. a) Space-filling representation of tetrameric columnar stack from single crystal x-ray diffraction data. b) ORTEP of tetrameric columnar stack with molecules colored by symmetry equivalence showing the helical nature of the column. Thermal ellipsoids are shown at 50% probability, and H atoms are omitted for clarity.

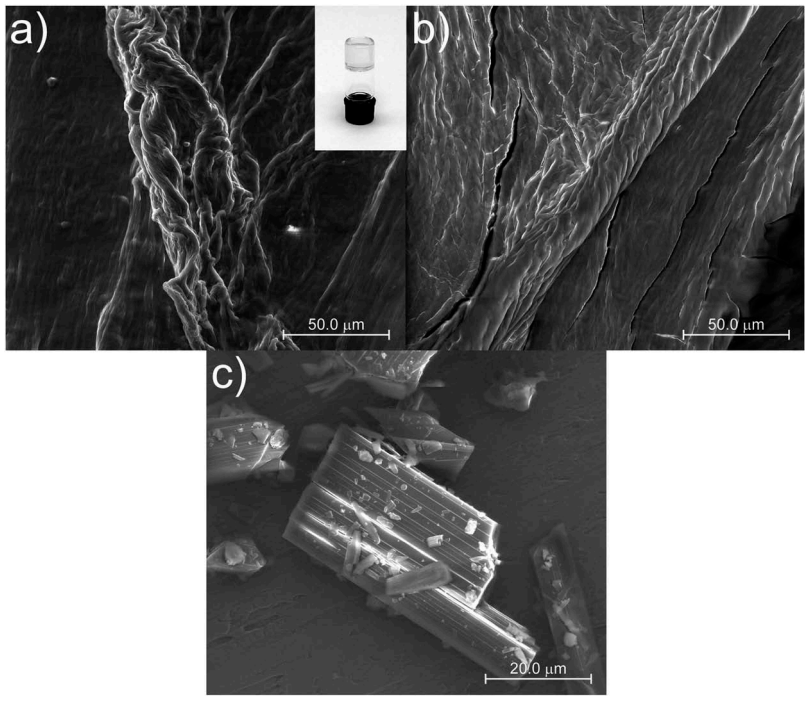

Figure 5. VP-SEM images of a) **1a** (*S*)-BINABarb $CHCl_3$ gel with inset of an inverted vial containing the gel, b) **1b** (*R*)-BINABarb $CHCl_3$ gel, c) crystalline solid of **1b.**

bonding motif by strong H-bond donors and acceptors interrupts dimerization of the barbiturate and thus prevents the growth of one-dimensional fibers.

To further investigate the supramolecular ordering at the microscale level, we used a variable pressure scanning electron microscopy (VP-SEM) to visualize the type of microstructures (tapes, ribbons, sheets, fibers, coils, etc.) that were formed. Figure 5 shows the difference between the microcrystalline material before dissolution in $CHCl_3$ and the supramolecular fibers formed from either (*S*)-BINABarb or (*R*)-BINABarb. These fibers showed a diverse size range from 3–15 µm in diameter with various levels of entanglement. Notably, the images clearly show microstructures with helical twists, demonstrating that the axial molecular chirality of the individual subunits is translated into microstructures.

Conclusions

In conclusion, we report the first chiral barbiturate to act as a single-component LMOG. This new LMOG can be classified as a super gelator and is capable of gelating a variety of chlorinated and aromatic solvents. The structural requirements for gelation when compared to other non-gelating analogs appear to be both a polar H-bonding head group and chiral aromatic backbone. VP-SEM and XRD experiments show the self-assembly of **1** results in the production of fiber type microstructures likely promoted by the dimerization of individual barbiturate units. Potential applications of this new LMOG include use as chiral dopants for liquid crystals and use as chiral shift/transfer reagents. These, as well as other potential applications, are currently being investigated by our laboratory.

Experimental details

General

All commercially-available reagents were used as received. Anhydrous, deoxygenated solvents were collected from a Pure Process Technologies solvent purification system. Reactions were monitored using Merck F_{254} silica gel 60 TLC plates and visualized using UV light or a $KMnO_4$ stain. Chromatographic purification was performed using a Biotage automated flash chromatography purification system. ^{1}H and $^{13}C\{^{1}H\}$ NMR spectra were recorded at the reported frequencies, and chemical shifts are reported in ppm (δ) and referenced to the residual solvent resonance. All ^{19}F spectra were indirectly referenced via the Bruker TopSpin 3.5 software suite to $CFCl_3$. The following naming conventions were used to describe NMR couplings: (s) singlet, (d) doublet, (t) triplet, (q) quartet, (dd) doublet of doublets, (m) multiplet, (b) broad.

Synthesis

Dibromomethylbinapthalene precursors were prepared according to scheme S1 using a modified procedure as reported by Ooi et al. The resultant compounds had spectroscopic signals that matched the reported data (50).

2,2′-bis(trifluoromethanesulfonyloxy)-1,1′-binaphthyl, **[(*R*)-I]**. (*R*)-BINOL (2.01 g, 7.02 mmol), *N*-phenylbistrifluormethanesulfonamide (5.02 g, 14.1 mmol), DIPEA (3.60 mL, 21.7 mmol) were combined in 10 mL dry DMF and stirred at r.t. for 24 hours. The reaction was diluted with Et_2O, washed 3x with H_2O and then with brine. The organic layer was dried over MgSO, filtered and concentrated under vacuum. The crude product was purified by column chromotography using hexanes:EtOAc gradiant (0% – 20%) as the eluent (R_f = 0.12, Hex; R_f = 0.45, 20% EtOAc) to yield the final product as an oil that solidifies to a white solid upon standing (3.27 g, 85%) ^{1}H NMR (500 MHz, $CDCl_3$) δ: 8.15 (d, *J* = 9.1 Hz, 2H), 8.02 (d, *J* = 8.3 Hz, 2H), 7.66–7.57 (m, 4H), 7.43 (t, *J* = 7.6 Hz, 2H), 7.32–7.19 (m, 2H). $^{13}C\{^1H\}$ NMR (126 MHz, $CDCl_3$) δ: 145.51, 133.27, 132.48, 132.12, 128.48, 128.11, 127.45, 126.88, 123.57, 119.46, 118.26 (q, *J* = 320.7 Hz). ^{19}F NMR (471 MHz, $CDCl_3$) δ: −74.56.

2,2′-bis(trifluoromethanesulfonyloxy)-1,1′-binaphthyl, **[(*S*)-I]**. Was prepared similar to **(*R*)-I** using the following amounts: (S)-BINOL (996 mg, 3.48 mmol), *N*-phenylbistrifluormethanesulfonamide (2.50 g, 7.00 mmol), DIPEA (1.8 mL, 10 mmol) in 5 mL DMF. The product was isolated as a white solid (1.35 g, 71%). ^{1}H NMR (500 MHz, $CDCl_3$) δ: 8.15 (d, *J* = 9.1 Hz, 2H), 8.01 (d, *J* = 8.3 Hz, 2H), 7.62 (d, *J* = 9.1 Hz, 2H), 7.59 (ddd, *J* = 8.1, 6.7, 1.0 Hz, 2H), 7.42 (ddd, *J* = 8.2, 6.8, 1.2 Hz, 2H), 7.32–7.19 (m, 2H). $^{13}C\{^1H\}$ NMR (126 MHz, $CDCl_3$) δ: 145.51, 133.28, 132.48, 132.12, 128.48, 128.11, 127.45, 126.89, 123.57, 119.53, 118.26 (q, *J* = 320.7). ^{19}F NMR (471 MHz, $CDCl_3$) δ: −74.57.

(*R*)-2,2′-Dimethyl-1,1′-binaphthyl, **[(*R*)-II]. (*R*)-I** (2.502 g, 4.54 mmol) and $NiCl_2$(dppp) (82.0 mg, 0.139 mmol) were combined in a Schlenk and evacuated/refilled 3x with and atmosphere of N_2. Dry and degassed Et_2O (25 mL) was added via cannula and cooled to 0 °C. MeMgI (2 M in Et_2O, 6.8 mL, 14 mmol) was added slowly. The reaction mixture was then heated to reflux and stirred for 19 hours. The reaction was then cooled to 0 °C and quenched with 2 mL of 1 M HCl (aq), diluted with Et_2O, and filtered through celite. The organic layer was then washed 3x with H_2O and brine, dried over $MgSO_4$, filtered, and concentrated under vacuum. The crude mixture was dissolved in hexanes and the risdual salts removed via filtration. The product was purified using column chromotograpny using hexanes as the eluent (R_f = 0.23) to yield the final product as a colorless oil that solidifies upon standing (1.08 g, 84%). ^{1}H NMR (500 MHz, $CDCl_3$) δ: 7.89 (t, *J* = 8.0 Hz, 4H), 7.51 (d, *J* = 8.4 Hz, 2H), 7.39 (t, *J* = 7.5 Hz, 2H), 7.21 (t, *J* = 7.6 Hz, 2H), 7.05 (d, *J* = 8.5 Hz, 2H), 2.04 (s, 6H). ^{13}C NMR (126 MHz, $CDCl_3$) δ: 135.26, 134.42, 132.89, 132.35, 128.86, 128.06, 127.56, 126.21, 125.78, 125.02, 20.18.

(*S*)-2,2′-Dimethyl-1,1′-binaphthyl, **[(*S*)-II]**. Was prepared similar to **(*R*)-2** using the following amounts: **(*S*)-I** (4.86 g, 8.83 mmol), $NiCl_2$(dppp) (157 mg, 0.265 mmol), degassed Et_2O (40 mL), MeMgI (2 M in Et_2O, 13 mL, 26 mmol). The final product was isolated as an oil that solidified upon standing (2.185 g, 88%) ^{1}H NMR (500 MHz, $CDCl_3$) δ: 7.89 (t, *J* = 8.0 Hz, 4H), 7.51 (d, *J* = 8.4 Hz, 2H), 7.39 (ddd, *J* = 8.1, 6.6, 1.1 Hz, 2H), 7.21 (ddd, *J* = 8.2, 6.8, 1.3 Hz, 2H), 7.05 (d, *J* = 8.4 Hz, 2H), 2.04 (s, 6H). $^{13}C\{^1H\}$ NMR (126 MHz, $CDCl_3$) δ: 135.27, 134.43, 132.90, 132.36, 128.86, 128.06, 127.57, 126.22, 125.78, 125.03, 20.18.

(*R*)-2,2′-Bis(bromomethyl)-1,1′-binaphthyl, **[(*R*)-III]. (*R*)-II** (428 mg, 1.52 mmol), *N*-bromosuccinimide (594 mg, 3.34 mmol), and AIBN (24.3 mg, 0.148 mmol, 10%) were dissolved in benzene (15 mL) and heated to reflux for 3 hours. The reaction was cooled to room temperature and diluted with Et_2O. The organic layer was washed 3x with H_2O, 3x brine, dried over $MgSO_4$ and filtered. The crude product was purified using column chromotography (R_f = 0.23, Hex). The combined fractions were concentrated and the product was triturated in hexanes and then filtered to yield the final product as a white solid (302 mg, 45%) ^{1}H NMR (500 MHz, $CDCl_3$) δ: 8.02 (d, *J* = 8.6 Hz, 2H), 7.93 (d, *J* = 8.2 Hz, 2H), 7.75 (d, *J* = 8.6 Hz, 2H), 7.49 (ddd, *J* = 8.2, 6.7, 1.0 Hz, 2H), 7.32–7.18 (m, 2H), 7.08 (d, *J* = 8.5 Hz, 2H), 4.26 (s, 4H). $^{13}C\{^1H\}$ NMR (126 MHz, $CDCl_3$) δ: 134.33, 134.23, 133.41, 132.66, 129.52, 128.17, 127.89, 126.99, 126.97, 126.94, 32.78.

(*S*)-2,2′-Bis(bromomethyl)-1,1′-binaphthyl, **[(*S*)-III]**. Was prepared similar to **(*R*)- III** using the following amounts: **(*S*)-II** (501 mg, 1.77 mmol), *N*-bromosuccinimide (668 mg, 3.75 mmol), and AIBN (32.0 mg, 0.195 mmol), and benzene(15 mL). After 3 hours 125 mg (0.702 mmol) NBS and 5.0 mg (3.0 µmol) AIBN were added and heated to reflux for an additional hour. The final product was isolated as a white solid (294 mg, 38%). ^{1}H NMR (500 MHz, $CDCl_3$) δ: 8.02 (d, *J* = 8.6 Hz, 2H), 7.93 (d, *J* = 8.2 Hz, 2H), 7.75 (d, *J* = 8.6 Hz, 2H), 7.49 (t, *J* = 7.5 Hz, 2H), 7.28 (t, *J* = 7.9 Hz, 2H), 7.08 (d, *J* = 8.5 Hz, 2H), 4.26 (s, 4H). ^{13}C NMR (126 MHz, $CDCl_3$) δ: 134.33, 134.23, 133.40, 132.65, 129.51, 128.17, 127.89, 126.99, 126.96, 126.94, 32.78.

General synthesis of barbituric acid derivatives 1–3

To a solution of barbituric acid (1 equiv.) in DMSO was added diisopropylethylamine (DIPEA, 2.3 equiv.) The mixture was stirred at room temperature for 10 min,

after which time a precipitate formed (depending on the concentration of barbituric acid). The corresponding benzyl bromide (2 equiv.) was then added to the mixture, which was then heated to 50°C and stirred overnight (~22 h). The crude, clear orange reaction mixture was diluted with H_2O and extracted 3x with EtOAc. The combinded organic extracts were washed 3x with brine, dried over $MgSO_4$, filtered and concentrated. The residue was triturated with a DCM:hexanes mixture and the resulting solids collected via vacuum filtration to yield the final product. In general, this gave acceptably pure product. Further purification could be achieved via recrystallization from EtOH or column chromatography.

5,5′-(*S*)-1,1′-binaphthylbarbituric acid **[(*S*)-BINABARB, (1a)]**: This compound was prepared as described in the general procedure using the following quantities barbituric acid (49.7 mg, 0.388 mmol) in 5 mL DMSO, DIPEA (160 µL, 0.92 mmol), and **(*S*)-III** (172 mg, 0.391 mmol). The compound was purified by column chromatography (R_f = 0.33, 1:1 EtOAc:Hex) followed by recrystallization from ethanol to yield the final product as a white solid (36 mg, 23%). ^{1}H NMR (500 MHz, DMSO-d_6) δ: 11.14 (s, 2H), 8.01 (d, *J* = 8.2 Hz, 2H), 7.95 (d, *J* = 8.3 Hz, 2H), 7.50 (d, *J* = 8.4 Hz, 2H), 7.47 (t, *J* = 7.5 Hz, 2H), 7.25 (t, J = 7.6 Hz, 2H), 7.08 (d, *J* = 8.6 Hz, 2H), 3.09 (d, *J* = 13.6 Hz, 2H), 2.97 (d, *J* = 13.5 Hz, 2H). ^{13}C NMR (126 MHz, DMSO-d_6) δ: 172.22, 150.36, 134.23, 132.77, 132.63, 130.93, 129.78, 128.23, 127.35, 126.29, 125.69, 125.24, 62.05. HRMS (ESI-TOF) *m/z*: $[M + Na]^+$ Calcd for $C_{26}H_{19}N_2O_3$, 407.1396; found 407.1396.

5,5′-(*R*)-1,1′-binaphthylbarbituric acid **[(*R*)-BINABARB, (1b)]**: This compound was prepared as described in the general procedure using the following quantities: barbituric acid (57.9 mg, 0.452 mmol) in 3 mL DMSO, DIPEA (180 µL, 1.0 mmol), and **(*R*)-III** (199 mg µL, 0.452 mmol). The compound was purified by column chromatography (R_f = 0.33, 1:1 EtOAc:Hex) followed by recrystallization from ethanol to yield the final product as a white solid (62 mg, 33%) ^{1}H NMR (500 MHz, DMSO-d_6) δ: 11.14 (s, 2H), 8.01 (d, *J* = 8.2 Hz, 2H), 7.95 (d, *J* = 8.4 Hz, 2H), 7.50 (d, *J* = 8.4 Hz, 2H), 7.47 (t, *J* = 7.5 Hz, 2H), 7.25 (t, *J* = 7.6 Hz, 2H), 7.08 (d, *J* = 8.5 Hz, 2H), 3.09 (d, *J* = 13.5 Hz, 2H), 2.97 (d, *J* = 13.5 Hz, 2H). ^{13}C NMR (126 MHz, DMSO-d_6) δ: 172.22, 150.37, 134.23, 132.76, 132.63, 130.92, 129.78, 128.23, 127.35, 126.28, 125.69, 125.24, 62.04, 38.09. HRMS (ESI-TOF) *m/z*: $[M + Na]^+$ Calcd for $C_{26}H_{19}N_2O_3$, 407.1396; found 407.1385.

5,5′-dibenzylbarbituric acid **(3)**: This compound was prepared as described in the general procedure using the following quantities: barbituric acid (253 mg, 1.95 mmol) in 5 mL DMSO, DIPEA (780 uL, 4.45 mmol), and benzyl bromide (470 µL, 3.95 mmol). The product was isolated as a white solid (474 mg, 78%). ^{1}H NMR (500 MHz, DMSO-d_6) δ: 11.19 (s, 2H), 7.35–7.17 (m,6), 7.11–7.01 (m, 4H), 3.28 (s, 4H). ^{13}C{^{1}H} NMR (126 MHz, DMSO-d_6) δ: 171.99, 148.85, 135.13, 129.26, 128.47, 127.33, 58.99, 43.78.

Determining gelation behavior

A 25 mM sample of the numbered compound was prepared in the desired solvent. The sample was sonicated and heated in a GC-vial to reflux or until all visible solids were dissolved. The sample was then allowed to cool and stand for at least 10 minutes before being inverted. If the sample appeared homogenous and no flow was observed, then the solvent and compound combination was marked as a gel.

Sample preparation for DOSY NMR

For control compounds **2** and **3**, a corresponding amount of a concentrated stock solution was diluted with $CDCl_3$ to a total volume of 600 µL to achieve the desired concentrations. For the (*S*)-BINABarb samples ≤ 10 mM, a similar procedure to that of **2** and **3** was used. For the more concentrated samples of (*S*)-BINABarb, a corresponding amount of solid was added to an NMR tube and dissolved in $CDCl_3$ to achieve the desired concentration with a total volume of 600 µL. Heating and sonication was necessary to achieve complete dissolution of the more concentrated samples. The samples were then allowed to cool to room temperature and stand for at least 15 minutes prior analysis.

Determination of diffusion coefficients

Diffusion-ordered spectroscopy (DOSY) was performed on a 600 MHz Bruker spectrometer with a prodigy cryoprobe using the **ledbpgp2s** pulse sequence. The 90° pulse widths were optimized individually for each sample. A typical experiment has a Δ (d20) = 0.060 s, δ (p30*2) = 3.0 ms with a varying gradient strength between 35–45% with data taken in 25 increments. All data was processed in MestReNova using the max peak height method for the doublet centered at 3.40 ppm (Bn H) with the following values: γ = 42.58 (MHz T^{-1}), k = 6.57 (DAC to G), Δ = 0.060 s, δ = 3.0 ms. The exponential decays were then fit using the three parameter exponential fit function in the MestReNova data analysis package. The data reported represents the average of at least 3 or more trials, and the reported uncertainty is the standard deviation.

Determination of diffusion coefficients for VT DOSY

Variable temperature diffusion-ordered spectroscopy (VT DOSY) was performed on a 500 MHz Varian spectrometer

using the **DONESHOT** pulse sequence. A 20 mM sample in $CDCl_3$ was prepared similarly to the room temperature samples. A typical experiment has a $\Delta = 0.050$ s, $\delta = 2.0$ ms with the low and high pulse gradients set to 2,000 and 22,000, respectively. The temperature was incrementally increased up to 50°C and allowed to equilibrate for at least 10 minutes before each acquisition (black squares). After the acquisition at 50°C, the sample was then re-cooled inside the spectrometer to 25°C and the diffusion coefficient was remeasured (red circle). All data was processed in MestReNova using the max peak height method for the doublet centered at 3.40 ppm (Bn Hs) with the following values: $\gamma = 26{,}752.2205$ (G^{-1} s^{-1}), $k = 0.00222$, $\Delta = 0.05$ s, $\delta = 2.0$ ms. The exponential decays were then fit using the three parameter exponential fit function in the MestReNova data analysis package.

Variable pressure- scanning electron microscopy details

To image the gels, an FEI Quanta 200 ESEM was used in variable-pressure mode. The best image quality was obtained operating at 100pa pressure, while actively cooling the gel to 4°C (resulting in 12% relative humidity). Images were captured at 15 kV, using spot size 4, with a GSED (gaseous-state electron detector.) Samples were prepared for SEM imaging by placing several micro-liters of fully hydrated/solvated gel onto cooled aluminum pucks, which were placed onto an FEI Peltier-cooled stage.

Acknowledgments

This work was supported by the NSF (CHE-1506221). NMR, SEM, and MS facilities at CAMCOR/UO are supported by the NSF (CHE-0923589, CHE-1427987, CHE-0521653, and CHE-1625529). We thank Jackie McGrath for early synthetic work, Erik Leonhert for help with initial electron microscopy experiments, and Justin Barry for help with initial DOSY experiments.

Disclosure statement

No potential conflict of interest was reported by the authors.

Funding

This work was supported by the National Science Foundation [CHE-0521653,CHE-0923589,CHE-1427987,CHE-1506221,CHE-1625529].

References

(1) Steed, J.W.;. *Chem. Commun.* **2011**, *47*(5), 1379–1383.
(2) Murata, K.; Aoki, M.; Nishi, T.; Ikeda, A.; Shinkai, S. *J. Chem. Soc. Chem. Commun.* **1991**, *24*, 1715–1718.
(3) Pozzo, J.L.; Clavier, G.M.; Desvergne, J.P. *J. Mater. Chem.* **1998**, *8*(12), 2575–2577.
(4) Haines, S.R.; Harrison, R.G. *Chem. Commun.* **2002**, *23*, 2846–2847.
(5) Ayabe, M.; Kishida, T.; Fujita, N.; Sada, K.; Shinkai, S. *Org. Biomol. Chem.* **2003**, *1*(15), 2744–2747.
(6) Sugiyasu, K.; Fujita, N.; Takeuchi, M.; Yamada, S.; Shinkai, S. *Org. Biomol. Chem.* **2003**, *1*(5), 895–899.
(7) de Jong, J.J.D.; Lucas, L.N.; Kellogg, R.M.; van Esch, J.H.; Feringa, B.L. *Science*. **2004**, *304*(5668), 278–281.
(8) Chen, X.; Huang, Z.; Chen, S.Y.; Li, K.; Yu, X.Q.; Pu, L. *J. Am. Chem. Soc.* **2010**, *132*(21), 7297–7299.
(9) Ran, X.; Gao, Q.Q.; Zhang, Y.; Guo, L.J. RSC Adv. **2017**, *7* (88), 56016–56022.
(10) Kartha, K.K.; Babu, S.S.; Srinivasan, S.; Ajayaghosh, A. *J. Am. Chem. Soc.* **2012**, *134*(10), 4834–4841.
(11) Liu, Q.T.; Wang, Y.L.; Li, W.; Wu, L.X. *Langmuir*. **2007**, *23* (15), 8217–8223.
(12) Jones, C.D.; Steed, J.W. *Chem. Soc. Rev.* **2016**, *45*(23), 6546–6596.
(13) Piepenbrock, M.O.M.; Lloyd, G.O.; Clarke, N.; Steed, J.W. *Chem. Rev.* **2010**, *110*(4), 1960–2004.
(14) Duan, P.F.; Yanai, N.; Nagatomi, H.; Kimizuka, N. *J. Am. Chem. Soc.* **2015**, *137*(5), 1887–1894.
(15) Friggeri, A.; Gronwald, O.; van Bommel, K.J.C.; Shinkai, S.; Reinhoudt, D.N. *J. Am. Chem. Soc.* **2002**, *124*(36), 10754–10758.
(16) An, B.K.; Lee, D.S.; Lee, J.S.; Park, Y.S.; Song, H.S.; Park, S. Y. *J. Am. Chem. Soc.* **2004**, *126*(33), 10232–10233.
(17) Cardolaccia, T.; Li, Y.J.; Schanze, K.S. *J. Am. Chem. Soc.* **2008**, *130*(8), 2535–2545.
(18) Kishimura, A.; Yamashita, T.; Aida, T. *J. Am. Chem. Soc.* **2005**, *127*(1), 179–183.
(19) Kitamura, T.; Nakaso, S.; Mizoshita, N.; Tochigi, Y.; Shimomura, T.; Moriyama, M.; Ito, K.; Kato, T. *J. Am. Chem. Soc.* **2005**, *127*(42), 14769–14775.
(20) Puigmarti-Luis, J.; Laukhin, V.; Del Pino, A.P.; Vidal-Gancedo, J.; Rovira, C.; Laukhina, E.; Amabilino, D.B. *Angew. Chem. Int. Ed.* **2007**, *46*(1–2), 238–241.
(21) Lee, D.C.; McGrath, K.K.; Jang, K. *Chem. Commun.* **2008**, *31*, 3636–3638.
(22) Ajayaghosh, A.; Praveen, V.K. *Accounts Chem. Res.* **2007**, *40*(8), 644–656.
(23) Ajayaghosh, A.; Praveen, V.K.; Vijayakumar, C. *Chem. Soc. Rev.* **2008**, *37*(1), 109–122.
(24) Vintiloiu, A.; Leroux, J.C. *J. Control. Release*. **2008**, *125*(3), 179–192.
(25) Sangeetha, N.M.; Maitra, U. *Chem. Soc. Rev.* **2005**, *34* (10), 821–836.
(26) Kimura, M.; Kobayashi, S.; Kuroda, T.; Hanabusa, K.; Shirai, H. *Adv. Mater.* **2004**, *16*(4), 335–338.
(27) Simmons, B.; Li, S.C.; John, V.T.; McPherson, G.L.; Taylor, C.; Schwartz, D.K.; Maskos, K. Nano Lett. **2002**, *2*(10), 1037–1042.
(28) Hirst, A.R.; Escuder, B.; Miravet, J.F.; Smith, D.K. *Angew. Chem. Int. Ed.* **2008**, *47*(42), 8002–8018.
(29) Svobodova, H.; Noponen, V.; Kolehmainen, E.; Sievanen, E. RSC Adv. **2012**, *2*(12), 4985–5007.
(30) Hirst, A.R.; Smith, D.K. *Chem. Eur. J.* **2005**, *11*(19), 5496–5508.

(31) Draper, E.R.; Adams, D.J. *Chem. Soc. Rev.* **2018**, *47*(10), 3395–3405.
(32) Buerkle, L.E.; Rowan, S.J. *Chem. Soc. Rev.* **2012**, *41*(18), 6089–6102.
(33) Abdallah, D.J.; Weiss, R.G. *Adv. Mater.* **2000**, *12*(17), 1237–1247.
(34) Hanabusa, K.; Miki, T.; Taguchi, Y.; Koyama, T.; Shirai, H. *J. Chem. Soc. Chem. Commun.* **1993**, *18*, 1382–1384.
(35) Jeong, S.W.; Murata, K.; Shinkai, S. *Supramol. Sci.* **1996**, *3* (1), 83–86.
(36) Inoue, K.; Ono, Y.; Kanekiyo, Y.; Ishi-i, T.; Yoshihara, K.; Shinkai, S. *J. Org. Chem.* **1999**, *64*(8), 2933–2937.
(37) Yagai, S.; Higashi, M.; Karatsu, T.; Kitamura, A. *Chem. Mat.* **2004**, *16*(19), 3582–3585.
(38) Yagai, S.; Nakajima, T.; Kishikawa, K.; Kohmoto, S.; Karatsu, T.; Kitamura, A. *J. Am. Chem. Soc.* **2005**, *127* (31), 11134–11139.
(39) Schmidt, R.; Stolte, M.; Grune, M.; Wurthner, F. *Macromolecules*. **2011**, *44*(10), 3766–3776.
(40) Brizard, A.; Oda, R.; Huc, I. Chirality Effects in Self-Assembled Fibrillar Networks. In *Low Molecular Mass Gelator*; Springer Berlin Heidelberg: Berlin, Heidelberg, 2005; pp 167–218.
(41) Smith, D.K.;. *Chem. Soc. Rev.* **2009**, *38*(3), 684–694.
(42) Ajayaghosh, A.; Varghese, R.; George, S.J.; Vijayakumar, C. *Angew. Chem. Int. Ed.* **2006**, *45*(7), 1141–1144.
(43) Cai, W.; Wang, G.T.; Du, P.; Wang, R.X.; Jiang, X.K.; Li, Z.T. *J. Am. Chem. Soc.* **2008**, *130*(40), 13450–13459.
(44) Das, R.K.; Kandanelli, R.; Linnanto, J.; Bose, K.; Maitra, U. *Langmuir*. **2010**, *26*(20), 16141–16149.
(45) Hifsudheen, M.; Mishra, R.K.; Vedhanarayanan, B.; Praveen, V.K.; Ajayaghosh, A. *Angew. Chem. Int. Ed.* **2017**, *56*(41), 12634–12638.
(46) Sun, Y.; Li, S.; Zhou, Z.; Saha, M.L.; Datta, S.; Zhang, M.; Yan, X.; Tian, D.; Wang, H.; Wang, L.; Li, X.; Liu, M.; Li, H.; Stang, P.J. *J. Am. Chem. Soc.* **2018**, *140*(9), 3257–3263.
(47) Bielejewski, M.; Kowalczuk, J.; Kaszynska, J.; Lapinski, A.; Luboradzki, R.; Demchuk, O.; Tritt-Goc, J. *Soft Matter*. **2013**, *9*(31), 7501–7514.
(48) Hisamatsu, Y.; Banerjee, S.; Avinash, M.B.; Govindaraju, T.; Schmuck, C. *Angew. Chem. Int. Ed.* **2013**, *52*(48), 12550–12554.
(49) Murata, K.; Aoki, M.; Suzuki, T.; Harada, T.; Kawabata, H.; Komori, T.; Ohseto, F.; Ueda, K.; Shinkai, S. *J. Am. Chem. Soc.* **1994**, *116*(15), 6664–6676.
(50) Ooi, T.; Kameda, M.; Maruoka, K. *J. Am. Chem. Soc.* **2003**, *125*(17), 5139–5151.